Accepted Manuscript

Point-of-need simultaneous electrochemical detection of lead and cadmium using low-cost stencil-printed transparency electrodes

Daniel Martín-Yerga, Isabel Álvarez-Martos, M.Carmen Blanco-López, Charles S. Henry, M.Teresa Fernández-Abedul

PII: S0003-2670(17)30692-X

DOI: 10.1016/j.aca.2017.05.027

Reference: ACA 235237

To appear in: *Analytica Chimica Acta*

Received Date: 8 February 2017

Revised Date: 21 May 2017

Accepted Date: 31 May 2017

Please cite this article as: D. Martín-Yerga, I. Álvarez-Martos, M.C. Blanco-López, C.S. Henry, M.T. Fernández-Abedul, Point-of-need simultaneous electrochemical detection of lead and cadmium using low-cost stencil-printed transparency electrodes, *Analytica Chimica Acta* (2017), doi: 10.1016/j.aca.2017.05.027.

This is a PDF file of an unedited manuscript that has been accepted for publication. As a service to our customers we are providing this early version of the manuscript. The manuscript will undergo copyediting, typesetting, and review of the resulting proof before it is published in its final form. Please note that during the production process errors may be discovered which could affect the content, and all legal disclaimers that apply to the journal pertain.

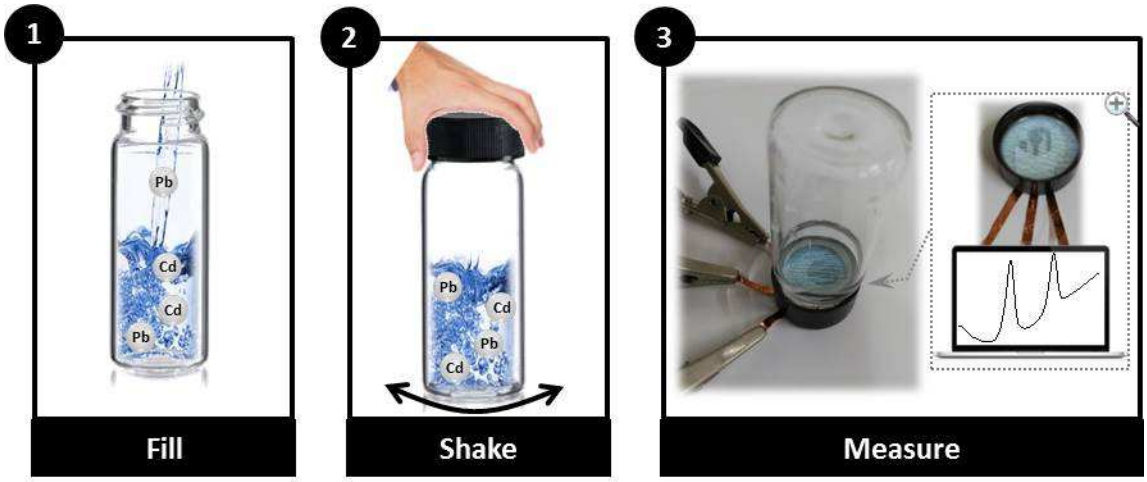

ACCEPTED MANUSCRIPT

ACCEPTED MANUSCRIPT

Point-of-need simultaneous electrochemical detection of lead and cadmium using low-cost stencil-printed transparency electrodes

Daniel Martín-Yerga[#1], *Isabel Álvarez-Martos*[#2], *M.Carmen Blanco-López*[1], *Charles S. Henry**[3], *M.Teresa Fernández-Abedul**[1]

[1] Departamento de Química Física y Analítica, Universidad de Oviedo, 33006 Oviedo, Spain

[2] Interdisciplinary Nanoscience Center (iNANO), Aarhus University, 8000 Aarhus C, Denmark

[3] Department of Chemistry, Colorado State University, Ft. Collins CO80523, USA

[#] These authors contributed equally to this work

* Corresponding author: M. Teresa Fernández-Abedul
Departamento de Química Física y Analítica
Universidad de Oviedo
Julián Clavería 8, Oviedo 33006 (Spain)
E-mail: mtfernandeza@uniovi.es
Telephone: (+34) 985102968

* Corresponding author: Charles S. Henry
Department of Chemistry
Colorado State University
1872 Campus Delivery
Ft. Collins CO 80523 (USA)
E-mail: Chuck.Henry@colostate.edu
Telephone: (970) 491-2852

ACCEPTED MANUSCRIPT

ABSTRACT

In this work, we report a simple and yet efficient stencil-printed electrochemical platform that can be integrated into the caps of sample containers and thus, allows in-field quantification of Cd(II) and Pb(II) in river water samples. The device exploits the low-cost features of carbon (as electrode material) and paper/polyester transparency sheets (as substrate). Electrochemical analysis of the working electrodes prepared on different substrates (polyester transparency sheets, chromatographic, tracing and office papers) with hexaammineruthenium(III) showed that their electroactive area and electron transfer kinetics are highly affected by the porosity of the material. Electrodes prepared on transparency substrates showed the best electroanalytical performance for the simultaneous determination of Cd(II) and Pb(II) by square-wave anodic stripping voltammetry. Interestingly, the temperature and time at which the carbon ink was cured had significant effect on the electrochemical response, especially the capacitive current. The amount of Cd and Pb on the electrode surface can be increased about 20% by *in situ* electrodeposition of bismuth. The electrochemical platform showed a linear range comprised between 1 and 200 µg/L for both metals, sensitivity of analysis of 0.22 and 0.087 µA/ppb and limits of detection of 0.2 and 0.3 µg/L for Cd(II) and Pb(II), respectively. The analysis of river water samples was done directly in the container where the sample was collected, which simplifies the procedure and approaches field analysis. The developed point-of-need detection system allowedsimultaneous determination of Cd(II) and Pb(II) in those samples using the standard addition method with precise and accurate results.

KEYWORDS: paper-based devices, electroanalytical devices, transparency-film electrodes, low-cost electrodes, point-of-need detection, heavy metals

ACCEPTED MANUSCRIPT

1. INTRODUCTION

Heavy metals are considered one of the main sources of pollution in the environment. Among them, lead and cadmium represent a major concern for the public health due to their high toxicity even at low concentrations [1]. For this reason, the agencies that monitor our health safety maintain a strict policy on the maximum levels allowed in the different sources of human exposure. For instance, the guidelines of the World Health Organization set a safe threshold of Pb and Cd in drinking water below 10 and 3 µg/L, respectively [2]. Therefore, a highly-sensitive and accurate analysis of those heavy metals is necessary to minimize possible human and environmental exposure.

Electrochemical methods and especially anodic stripping voltammetry (ASV) have been widely used for their quantification with remarkable sensitivity, even at trace/ultratrace levels, due to the possibility of metal preconcentration on the electrode surface [3,4]. This approach allows short response time, miniaturization [5], portability and lower cost if compared to other techniques. The current trend towards on-site analysis also requires the replacement of conventional electrodes [6,7] by other miniaturized, low-cost and disposable alternatives, where the whole electrochemical cell is integrated in a millimeter device [8,9]. First generation electrodes made on glass, ceramic or polymeric substrates have started to be replaced by other more inexpensive and versatile, such as paper or plastic [10–12]. In recent years paper-based analytical devices (PADs) [13] gained popularity as they meet the so-called ASSURED (*i.e.* affordable, sensitive, specific, user-friendly, rapid and robust, equipment free, and deliverable to end-users) criteria described by the WHO.

Since Dungchai *et al.* demonstrated for the first time that electrochemistry can be coupled to PADs [14], numerous studies have used them to address different analytical issuess such as detection of glucose [15–17], ions [18], proteins [19], DNA [20], or heavy metals [21]. Methods employed for electrode preparation include stencil-printing, screen-printing and inkjet-printing [10]. Notice that there is not a single suitable technique therefore, its choice will depend on lateral resolution, thickness, homogeneity, speed, material or ink properties requirements [22], with this determining the overall electrochemical performance. In general, for metal detection bare carbon electrodes are not sufficiently sensitive and thus very often require modification [23]. In this sense, mercury films have worked extremely well, however, the trend towards green chemistry (*i.e.* reduce the use and generation of hazardous substances) [24] has led to their replacement by more environmental-friendly metals, such as bismuth or antimony. Since its introduction by Wang's group [25], bismuth (Bi) has been incorporated to electrodes in many

configurations. In bulk, where a bismuth precursor is added to the material before electrode fabrication, is more appropriate for carbon paste or screen-printed electrodes. Some successful examples include Bi nanoparticles [26], Bi_2O_3 [27] or Bi citrate [28]. Other more universal methods are physical deposition (drop-casting) [29], sputtering [30,31], or electrodeposition. In the later, Bi incorporation can be done either *ex situ* (Bi is electrodeposited in first place [32]) or *in situ* (Bi and the metals are simultaneously electrodeposited [33]).

In this paper, we developed a simple and yet efficient electrochemical platform that can be integrated into the caps of sample containers and thus, allows on-site quantification of Cd(II) and Pb(II) in river water samples. We stencil-printed carbon electrodes on several low-cost substrates: transparency sheets and chromatographic, tracing and office papers. As the Henry group pointed out, transparency sheets are, under some circumstances, better substrate candidates than paper itself, especially when dealing with electrochemical metal detection [23,34]. We performed in depth electrochemical analysis of the working electrodes and evaluate how the porosity of the material affects kinetics of electron transfer. By coupling the transparency-film electrodes with sample vial caps that can be in turn connected to the potentiostat, we provided here an innovative trace metal detection platform that allows quantification of Pb(II) and Cd(II) directly in the container where the samples are collected in a fast, sensitive and reliable way. We then used these systems, mounted on the caps of ordinary vials, to carry out anodic stripping voltammetry of Pb and Cd in water samples as a new example of the utility of this electrode format.

2. EXPERIMENTAL

2.1. Reagents and materials

Hexaammineruthenium(III) chloride, lead, cadmium and bismuth standards for ICP, iron(III) nitrate, copper(II) nitrate, cobalt(II) nitrate, nickel(II) nitrate and zinc(II) nitrate were acquired from Sigma-Aldrich. Bismuth(III) nitrate as well as acetic acid, sodium acetate and citric acid and were purchased from Merck. Carbon sensor paste (C10903P14) was purchased from Gwent Electronics. Adhesive copper tape was acquired from EMS (Electron Microscopy Sciences). All chemicals were of analytical grade.

Whatman No. 1 and P81 grade (with cellulose phosphate functional groups) chromatographic papers were purchased from Whatman (GE Healthcare Life Sciences). In order to simplify the notation, Whatman No.1 paper is named chromatographic paper and P81 grade named ionic

exchanger paper hereafter. Polyester transparency sheets (215 x 279 x 0.11 mm) were purchased from Highland 90. Navigator 100-g/m^2 office paper was purchased from a local supplier.

Solutions were prepared by using ultrapure water employing a Milli-Q Millipore water purification system. Heavy metal solutions were prepared daily by an appropriate dilution of standards in 0.1 M acetate buffer.

2.2. Instrumentation

A XEROX Colorqube 8570 printer was used to print the paper-based analytical devices following previously established protocols [23]. A RCT classic hot plate from IKA set at 105 ºC was used to melt the wax on the paper. Buffer solution pH was determined with a Crison micropH 2001 pH meter. Electrochemical measurements were performed employing a three-electrode system connected to an Autolab PGSTAT12 potentiostat (Metrohm) controlled by Autolab GPES 4.9 software. Electrodes were connected to the potentiostat by using a commercial screen-printed electrode connector (DRP-DSC, DropSens) and a 3-pin male connector with the aid of an insulated alligator clip as illustrated in the **Figure S1**.

2.3. Procedures

2.3.1. Mask fabrication

Polyester transparency sheets were used to fabricate the masks for stencil-printing. They were used as received and cut using a laser engraving system (Epilog, Golden, CO). The CO_2 laser system has a peak power of 30 W and was controlled by Epilog software after uploading drawing files. The pattern for transparency sheets was designed with CorelDRAW X5 software. The resulting masks were placed on top of the substrate (paper or transparency), previously fixed on the table with the aid of an adhesive tape.

2.3.2. SEM images

A JEOL 6610LV scanning electron microscope was used to characterize the working electrodes stencil-printed on transparency sheets. Images were recorded with the secondary electron detector and using an accelerated voltage of 20 kV.

2.3.3. Electrochemical cell and electrodes preparation

In the particular case of chromatographic paper circles of 10 mm diameter drawn with Inkscape software were printed with a wax printer (XEROX Colorqube 8570) and then placed on a hot plate at 100 ºC for 2 min to melt the wax, which lead to the hydrophobic barriers that constitute the electrochemical cell. After cool down to room temperature the stencil-printing process is started. For the rest of substrates, the electrochemical cell is just delimited with the aid of an insulating tape.

The protocol followed for stencil-printing the electrodes was the same for all substrates. First, the carbon paste was spread by hand over the surface with the aid of a squeegee. Then, the mask was carefully removed and the process was repeated in the x-y directions of the substrate sheets to fabricate a batch of tens of electrodes as can be seen in the **Figure S2** for a transparency sheet. Although in this work the electrodes were printed individually, this process can be automated allowing the electrodes to be mass-produced. The resulting stencil-printed electrodes were finally placed in an oven to remove any remaining solvent and stabilize the surface (curing step). Before any electrochemical measurement, adhesive tape was put in the backside of the paper substrates in order to avoid fluid leaking and improve the robustness of the devices.

In all devices, the working, reference and auxiliary electrodes were carbon-based and, therefore, the indicated potentials are related to the quasireference carbon electrode. A photograph of the electrodes fabricated on the different substrates is shown in **Figure 1** and a general scheme of the fabrication is presented in **Figure 2**.

[FIGURE 1]

[FIGURE 2]

2.3.4. Electrochemical measurements

Cyclic voltammetry (CV) measurements of $[Ru(NH_3)_6]^{3+}$ species in 0.1 M KCl were performed by scanning the potential between -0.2 and -0.8 V at different scan rates. A solution of 2.5 mM $[Ru(NH_3)_6]^{3+}$ was employed in all cases.

The detection of Cd(II) and Pb(II) was done by square-wave anodic stripping voltammetry (SWASV) with a preconcentration step of -1.4 V for 240 s. The square-wave scan was carried out afterwards from -1.4 to -0.4 V under these conditions: square wave amplitude of 25 mV, frequency of 20 Hz, step potential of 5 mV, and equilibration time of 10 s. Unless stated otherwise, a solution of 100 µg/L of Cd(II) and Pb(II) was used. All measurements were,

typically, performed by quintuplicate and at room temperature. The volume of the electrochemical cell was 70 µL for office paper, tracing paper and transparency sheets and 30 µL for chromatographic and ionic exchanger papers. The solutions were added to the paper electrodes on the same side where the cabon paste was deposited.

2.3.5. Incorporation of bismuth to the working electrode

Three different approaches were employed to incorporate bismuth into the working electrode of the transparency devices. Bulk modification, which consisted in mixing different amounts of $Bi(NO_3)_3$ with the commercial carbon paste before the stencil-printing process. After electrode fabrication, SWASV was carried out under the conditions described in the previous section. In this way, the Bi(III) precursor was reduced simultaneously to the preconcentration of Cd(II) and Pb(II). *Ex situ* bismuth electrodeposition, in which a 70 µL drop of Bi(III) in 0.1 M pH 4.5 acetate buffer was placed on top of the electrode surface and a negative potential of -1 V was applied for 90 s to reduce Bi(III) to Bi^0. The electrode surface was gently washed with ultrapure water and carefully dried with a paper towel before SWASV. *In situ* bismuth electrodeposition, done by addition of a specific concentration of Bi(III) to the Cd(II) and Pb(II) solution in which SWASV was performed.

2.3.6. Real sample analysis

The performance of transparency electrodes for the determination of Cd(II) and Pb(II) in real samples was assessed by analysis of two different water samples: i) river water from Morcín river (Asturias, Spain), near a coal mine, and ii) water from Avilés estuary (Asturias, Spain), near a metallurgical industry. The samples were collected and filtered *in situ* with a 0.45-µm filter paper to avoid any particulate matter, although they were visually clear. Measurements with the point-of-need device described in the following sectionswere performed by evaporation at room temperature of 5 µL of a 500 mg/L Bi(III) solution placed in the sample vial. Then, 5 mL of the water sample was collected and manually mixed with 68 mg of sodium acetate and 17 mg of citric acid salts. This allows us to work under the optimized experimental conditions of 0.1 M acetate buffer (pH 4.8) and 0.5 mg/L of Bi(III). Moreover, this approach is highly versatile as it allows the preparation of several sample vials with these salts that can be directly employed for point-of-need detection of aqueous samples. Initially Cd(II) and Pb(II) were not detected, therefore, the samples were spiked with known concentrations of these metals (10 and 50 µg/L), and the standard addition method was employed for the quantification with the point-of-need system.

3. RESULTS AND DISCUSSION

3.1. Electrochemical behavior of low-cost stencil-printed electrodes

The first aim of this work was to fully characterize the electrochemical performance of carbon electrodes stencil-printed on multiple paper types and transparency substrates. Electrodes were characterized in first place by cyclic voltammetry with $[Ru(NH_3)_6]^{3+}$ as redox indicator. The electrochemical detection of Cd(II) and Pb(II) by anodic stripping voltammetry was evaluated afterwards.

3.1.1. Cyclic voltammetry studies of low-cost stencil-printed electrodes

Stencil-printed electrodes fabricated on all substrates showed a well-defined couple of peaks characteristic of $[Ru(NH_3)_6]^{3+}$ (**Figure 3A**) with cathodic peak currents decreasing as follows -52±2, -41±3, -40±4, -31±3, and -26±4 (n=5) µA for chromatographic paper, transparency, office, tracing, and ionic exchanger papers. The peak potential differences between the cathodic and anodic peaks (ΔE_p) followed almost the opposite trend with values of 60±4, 70±4, 80±6, 82±6, and 145±12 (n=5) mV for chromatographic paper, transparency, tracing, office, and ionic exchanger papers. ΔE_p provides information about the electron transfer kinetics of the electrochemical process [35]. For a fast (reversible) process, a peak potential difference of 59/n mV is theoretically expected [36]. It seems that even though the electrodes are fabricated with the same material (carbon paste), the substrate has significant influence on $[Ru(NH_3)_6]^{3+}$ kinetics (typically a fast/reversible one-electron transfer process). It seems that kinetics of electron transfer are somehow improved by the more porous/fibrous nature of the chromatographic paper compared to the others, where the electrodes are just on the surface. Although the cationic exchanger paper was expected to provide better performance towards cationic species, it showed the highest ΔE_p and lowest peak currents so it was not used for the following studies. The same happened with tracing paper, which voltammetric response obtained at scan rates lower than 25 mVs^{-1} was well below the rest of evaluated substrates.

[FIGURE 3]

The reversibility of an electrochemical process and kinetic limitations or coupled reactions can be evaluated from the plot of ΔE_p and ratio of peak currents (i_{pc}/i_{pa}) against the scan rate. In line with above results, only the chromatographic paper approached the reversible peaks case with i_{pa}/i_{pc} close to 1 and ΔE_p close to the theoretically expected value of 59 mV, while the transparency and office paper deviated slightly (**Figure S3**). Therefore, this substrate provides

better electrochemical performance for the hexaammineruthenium reaction, which follows an outer-sphere one-electron transfer mechanism. At low scan rates, the i_{pa}/i_{pc} ratio is slightly lower than for high scan rates, a fact previously observed with other types of electrodes such as commercial screen-printed electrodes [37] and probably related to the reoxidation of $[Ru(NH_3)_6]^{2+}$ by oxygen [38], thereby decreasing its concentration and the anodic peak current.

The cyclic voltammograms recorded for the electrodes on office paper did not show highly defined peaks for low scan rates, but the faradaic processes of interest were defined when the scan rate increased (**Figure S4**). This may be due to absorption of the solution at longer times of analysis, which deteriorates the paper, or even to the generation of hydrogen bubbles, due to the hydrogen evolution reaction that starts at negative potentials close to those of the reaction. Analysis of the dependencies of the peak currents on the scan rate (**Figure S5**) showed that for transparency, chromatographic and office papers both cathodic and anodic peak currents increased linearly with the square root of scan rate ($v^{1/2}$), which denotes a diffusion-controlled eletron transfer reaction. Therefore, the voltammetric response can be assessed in terms of Randles-Sevcik equation (for a planar electrode at 25 ºC and a reversible process):

$$i_p = (2.69x10^5)\, n^{3/2}\, A\, C\, D^{1/2}\, v^{1/2} \qquad \textbf{(1)}$$

where i_p is the peak current intensity (A), n is the number of electrons transferred in the electrochemical reaction, A is the electrode area (cm^2), C is the bulk concentration of the analyte (mol/cm^3), D is the diffusion coefficient of the analyte (cm/s), and v is the scan rate (V/s). The electroactive area of the electrodes can thus be estimated according to eq. (1), as the rest of the parameters (n, D, C, v) are known ($D=9.1x10^{-6}$ cm^2/s, 0.1 M KCl) [39].

As the previous studies suggest, the area appears to be highly reliant on the substrate material and decreases following the tendency 0.109±0.005 (chromatographic paper), 0.086±0.004 (transparency), and 0.075±0.001 cm^2 (office paper). Obviously, the porous/fibrous nature of chromatographic paper allows absorption of part of the carbon paste, spreading it over the cellulose fibers and generating an area higher than for other substrates. It should also be considered its more hydrophilic nature, which enables adsorption of the solution added to the electrochemical cell, making contact with the inner cellulose fibers of the paper previously modified with carbon paste. In the case of hydrophobic substrates (*i.e.* transparency and office paper) the difference in electroactive area is minimal with a slightly higher value for transparency electrodes. It seems that even if the office paper could absorb part of the carbon

paste, the electrode surface behaves similarly to the transparency substrate, which does not absorb the carbon paste and the solution only makes superficial contact with the electrode.

For comparison, the geometric area of the electrodes was calculated to be about 0.13 cm^2 (see **Figure S6**). The difference between the estimated geometric area and the empirically obtained electroactive area can be explained due to nonconductive additives found in the commercial carbon paste or the pasivation of the carbon structure. It is difficult to know these substances as the composition of the commercial paste is proprietary information of the manufacturer, but it may contain several additives to improve the properties of the paste (viscosity, affinity to the substrate, etc.).

3.1.2. Anodic stripping voltammetry of Cd(II) and Pb(II) using low-cost stencil-printed electrodes

A very different response was observed in the square wave anodic stripping voltammograms (SWASV) recorded with electrodes on transparency, office and chromatographic papers (**Figure 3B**). Office paper showed no faradaic electrochemical processes and, despite maintaining a good contact with the solution for short-term measurements, the mechanical stability was compromised with time. Even when adhesive tape was put on the backside of the device, its robustness did not improve and therefore it does not seem to be a good choice for long-term measurements. The other two substrates show clear stripping signals for both Pb(II) and Cd(II) with comparable peak potentials and a small shift of 30-40 mV towards more positive potentials in case of chromatographic paper.

The amount of metal deposited on the electrode surface (Γ_{ads}) was estimated by integration of the total charge under the voltammetric peaks (Q_{ads}), according to the following equation:

$$Q_{ads} = nFA\Gamma_{ads} \quad \textbf{(2)}$$

where n is the number of exchanged electrons, F is the Faraday constant and A is the electroactive area of the electrode. For transparency substrates, the value of Γ_{ads} was found to be 39.2 nmol/cm^2 and 21.6 nmol/cm^2 for Cd and Pb respectively, which corresponds to a preconcentration of about 55% of the initial metal. The preconcentration efficiency was lower for chromatographic paper with about 44% and 51% and Γ_{ads} values of 10.9 nmol/cm^2 and 6.72 nmol/cm^2 for Cd and Pb respectively. Although the electroactive area is higher in this case,

since the only mass transport is diffusion, depletion of analytes in small pores could happen during the preconcentration time with this compromising sensitivity of analysis.

3.2. Optimization of the transparency electrode for lead and cadmium detection

3.2.1. Effect of the curing step in the anodic stripping response

The temperature and time at which the carbon paste is cured (curing step) after the stencil-printing process was critical for the good electrochemical performance of the transparency electrodes towards heavy metals. Several times and temperatures, such as 80 ºC (30, 60, 120 min) and at 37 ºC (1 to 15 days) were tested. Naturally, the evaporation of the solvents needed more time at lower temperatures. No significant differences were observed for the different times evaluated for the curing step at 80 ºC (**Figure S7A**), suggesting that 30 min were enough for solvent evaporation. Interestingly, when the devices were left at 37 ºC for longer times, the capacitive current of the electrochemical response gradually decreased, until becoming constant after 10 days. **Figure S11** shows the SEM images corresponding to day 1 and day 15 of curing. Reduction of the capacitive current was accompanied by a substantial increase of the stripping peak currents for Cd(II) and Pb(II) as shown in **Figure S7B**. The effect of the curing time at 37 ºC is significant as the capacitive current decreased by 70% (from 88 µA to 26 µA at -1V, approximately) and the stripping peak currents increased by almost 40% for both metals. Enhancement of the sensitivity is linked to the increase in the ratio between faradaic and capacitive currents. Then, after these studies, the transparency electrodes were allowed to cure for 10 days at 37 ºC before use in order to obtain devices with a better electrochemical response.

3.2.2. Bismuth effect on stripping currents

Certain metals form binary or multi-component alloys with bismuth (e.g. lead, cadmium, thallium or indium) [25,40], which helps to increase the amount deposited. In this study, the concentration of Pb(II) and Cd(II) was fixed constant and different methods of Bi(III) incorporation were evaluated (*i.e.* bulk modification, drop-casting and electrodeposition). The stripping currents of Pb(II) and Cd(II) increased with increasing concentration of Bi(III) until a maximum at 0.5 mg/L of Bi(III) where they start to decrease (**Figure 4**). This behavior has been attributed in the literature to the increasing number of nucleation sites, and therefore a more efficient alloy formation. However, when the Bi(III) concentration is too high, the film formed is thicker and the metallic preconcentration is less effective [41]. We can also observe that *in situ* Bi(III) deposition provided the highest stripping peak currents and therefore we moved forward with this approach and 0.5 mg/L Bi(III) concentration.

[FIGURE 4]

From the charge under the stripping peaks (**Figure S8**), we can estimate the amount of Pb(II) and Cd(II) on the surface to be 24.7 nmol/cm^2 and 50.1 nmol/cm^2, respectively, which corresponds to an increase of 14% and 28% compared to bare carbon electrodes. The interpretation of the shape of the stripping square-wave voltammetric responses (net, forward and backward components) can provide interesting information on the mechanism following the metal deposition onto the generated bismuth film. Mirceski *et al.* proposed three possible main mechanisms: i) simple anodic stripping mechanism (in a simplified way: reduction controlled by diffusion and oxidation controlled by adsorption), ii) anodic stripping mechanism coupled with adsorption and iii) anodic stripping mechanism with interactions [42]. In fact, background subtracted cyclic voltammograms (**Figure S9**) show that although the Pb(II) and Cd(II) diffusion coefficients are comparable and two electrons are transferred in both reactions, the net peak current for Cd is higher than this of Pb, with a i_p(Cd)/i_p(Pb) ratio of 3.0. This suggests that the reaction mechanism is indeed different.

For Cd, the peak of the forward component appears at a potential slightly more negative than the backward component, ~8 mV. Although both components have narrow peaks, the half-peak width is slightly higher for the backward peak component (39.0±1.0 *vs.* 35.5±0.9 mV, n=5), suggesting that diffusion has a greater effect in this case. For Pb, the peaks of the forward and backward components appeared at the same potential and the half-peak widths for the forward (29±1 mV) and backward (30±2 mV) components are slightly narrower than for Cd. The net peak is also narrower (41±1 mV for Cd *vs.* 35±1 mV for Pb), mainly due to peak potential differences in Cd components. We also analyzed the adsorption of metal ions according to $i_{p(forward)}/i_{p(backward)}$ ratio. The highest value obtained for Cd (2.31±0.06) compared to Pb (2.11±0.07) indicates that the adsorption of Pb(II) on the bismuth film is stronger than the adsorption of Cd(II), a fact also suggested by the narrower backward peak for Pb.

3.3. Analytical evaluation of transparency electrodes for Cd(II) and Pb(II) detection

3.3.1. Calibration plot

Parameters that can affect the stripping response, such as buffer pH (**Figure S10**), were evaluated in order to find the optimal operational conditions. Afterwards, calibration curves for the simultaneous determination of Pb(II) and Cd(II) were carried out in the range 1-200 ppb by

SWASV (**Figure 5**). The resulting plots were linear over the range assayed for both metals, following the equations $i_p(\mu A) = 0.6(\pm 0.1) + 0.22(\pm 0.02)$ [Cd(II)] (µg/L) (R^2=0.998) and $i_p(\mu A) = 0.1(\pm 0.1) + 0.087(\pm 0.004)$ [Pb(II)] (µg/L) (R^2=0.995) for Cd(II) and Pb(II), respectively. Limits of detection (LOD) estimated as the concentration corresponding to a signal that has a peak height equal to 3 times the standard deviation of the blank were 0.2 µg/L and 0.3 µg/L for Cd(II) and Pb(II), respectively. This LOD meets by far the legal requirements of <10 µg/L for Pb and <3 µg/L for Cd (WHO guidelines [2]). The analytical response of different devices was similar with a variation of the calibration slopes for same-day measurements of 7.5% and 4.8% (in terms of RSD, n=5) for Cd(II) and Pb(II), respectively. The inter-electrode precision evaluated from the voltammetric response of a 100 µg/L solution of Cd(II) and Pb(II) (n= 10 different devices) was 8.2% and 8.8% for Cd(II) and Pb(II), respectively. These overall results demonstrate the good reproducibility in fabrication of low-cost transparency electrodes (even being manually printed), so the use as disposable devices is completely reliable.

[FIGURE 5]

Importantly, simultaneous determination of Cd(II) and Pb(II) with the reported transparency electrodes seems to be the simplest and most reliable of the hitherto suggested bismuth-modified low-cost electrodes (**Table 1**) as well as most applicable for on-site analysis. The substrate used is usually cheaper because with a single transparency sheet tens of devices can be fabricated. This fact leads to cheap and disposable devices that can be used for the determination of very low concentrations of these metals. It is interesting to compare the performance of the device described here with a previous work in which transparency sheets were also employed as substrate and the working electrode was modified with graphene/polyaniline [23]. Although with comparable linear range and LOD, our device shows a significant sensitivity improvement (about 6X for Cd and more than 2X for Pb). The sensitivity is a very important analytical parameter, especially when trying to detect concentrations near the limit of detection. Moreover, the fabrication procedure reported here was faster, less tedious, and simpler as we did not use composite materials such as graphene/polyaniline. The enhanced sensitivity could be attributed to the use of different commercial carbon paste that leads to electrodes with higher electroactive area, as can noticed by comparing the peak currents for both devices. Therefore, the carbon paste is also a very important parameter that should be considered in the fabrication of devices, as it also happens for screen-printed electrodes [43].

[TABLE 1]

3.3.2. Interference study for Cd(II) and Pb(II) simultaneous determination

The possible interferences presented in solution by non-target metals such as Cu(II), Co(II), Zn(II), Fe(III) and Ni(II) were studied to evaluate the selectivity of the Cd(II) and Pb(II) simultaneous determination. A solution of 50 µg/L of Cd(II) and Pb(II) was employed, while the concentration of the non-target metals was varied (0.5-10 mg/L). The parameter employed to evaluate the interfering effect was the tolerance ratio [44], and a metal concentration modifying the peak current by > 12% was considered inhibitory. This value was chosen considering the reproducibility of the method previously estimated (~9% RSD). The tolerance ratio of the interfering species (**Table S1**) showed that under the working experimental conditions, the interference from metals such as Fe(III), Zn(II), Co(II) and Ni(II) until concentrations around 5-10 mg/L was insignificant. A greater interfering effect was found for Cu(II), with a tolerance ratio of 20 for 50 µg/L of Cd(II) and Pb(II). This may be due to the competition between copper and bismuth for surface sites in the electrodeposition step, as they do not form a metallic alloy [40]. However, this fact was not a problem for the real samples tested in this work, as demonstrated in the following section. If real samples with a high content in Cu(II) were analyzed, several strategies could be used in order to reduce this interference: ferrocyanide addition [45,46], Zn(II) addition (it is known that Zn and Cu form an intermetallic compound with ferrocyanide [47]), or selective complexation of the metals.

3.3.3. Electrochemical point-of-need detection in a sample vial

Transparency electrodes were integrated into the cap of sample vials in order to obtain a point-of-need system for portable detection. Electrodes were stencil-printed and the transparency sheets were properly cut to introduce them in the vial caps (with a circular geometry and septum). Then, the transparency sheet was attached with the aid of a small amount of adhesive glue on the inner surface of the septum. Adhesive copper tape was placed for electrode connection and extracted between the septum and the cap for the potentiostat connection *via* alligator clips. Insulating tape was precisely placed on the transparency to cover the connections and copper tape to prevent the contact with the solution. Thus, the electrodes were integrated into the caps as shown in the **Figure 6**. Salts were added as described in the Experimental section in order to have an appropriate buffer solution of 0.1 M acetate of pH 4.8 and 0.5 mg/L of Bi(III). After the addition of 5 mL of sample to the vial, the cap was placed onto the vial and the vial was turned upside down, so the solution could contact the electrode (**Figure 6C**). The copper strips were connected to the potentiostat with alligator clips and the measurement was performed. **Figure 6D** shows the voltammetric response under the optimized conditions for a

solution of 100 µg/L of Cd(II) and Pb(II). The use of citric acid (about 10 mM) to regulate the pH has no significant effect on the magnitude of the signal compared to using an acetic/acetate buffer solution. The point-of-need system allows the simultaneous and direct detection of heavy metals in a container that can be used to collect samples. Furthermore, the versatility and robustness of the transparency substrate leads to the easy fabrication of electrodes with different geometries that can be coupled to different containers and be used for direct electrochemical determination of other analytes. They could be attached to complex systems where other stages of the analytical process could be performed such as sample filtering or species separation. In addition, portable commercial or lab-made potentiostats may be ideal for using these point-of-need devices in field applications.

[FIGURE 6]

3.3.4. Simultaneous determination of Cd(II) and Pb(II) in river water samples

To evaluate the potential of the transparency electrodes for real sample analysis, two different water samples were tested: river water, from a river near a coal mine, and estuary water, near a metallurgical industry. Cadmium and lead levels were undetectable and, therefore, the samples were spiked with 10 and 50 µg/L of the metals to simulate polluted water. The analysis of these samples was performed using the standard addition method with the point-of-need system described in the previous section. Each sample was analyzed five times and the results obtained are shown in the **Table 2**. Recoveries ranged from 88 to 121% and the RSD (n = 5) was below 10%, indicating that the system is accurate and reproducible. These results show that both the transparency electrodes and the point-of-need system are suitable for the simultaneous determination of low concentrations of Cd(II) and Pb(II) in real samples with accuracy and precision, and could be used to detect contaminated samples.

[TABLE 2]

4. CONCLUSIONS

Herein, we reported stencil-printed electrodes fabricated on different low-cost substrates (*i.e.* polyester transparency sheets, chromatographic, tracing and office papers). We showed that porosity of the material affect the kinetics of electron transfer, being higher in the case of chromatographic paper. Electrodes fabricated on transparency sheets, office and chromatographic paper showed the best performance in terms of cyclic voltammetry, but transparency films were the most suitable for the detection of Pb(II) and Cd(II) at low concentrations. It was found that the curing step (time and temperature) and the modification

with a bismuth film have a significant effect on the signal/noise ratio. Good analytical performance (in terms of sensitivity, reproducibility, linear range) was found with these low-cost analytical devices and compares well with other electrodes previously described, with the advantage of having a lower manufacturing cost. The versatility and robustness of a substrate such as transparency sheets allowed the incorporation of electrodes into the cap of sample vials in order to analyze real samples directly in the container where the sample is collected. Simple stencil-printed bismuth-modified transparency electrodes have proven to be a suitable substrate for the fabrication of low-cost, disposable analytical devices for the determination of heavy metals in waters with the ability to employ them in point-of-need systems in field applications.

ACKNOWLEDGEMENTS

This work has been supported by the FC-15-GRUPIN-021 project from the Asturias Regional Government and the CTQ2014-58826-R project from the Spanish Ministry of Economy and Competitiveness (MINECO). Daniel Martín-Yerga thanks the MINECO for the award of a FPI grant (BES-2012-054408). Isabel Álvarez-Martos acknowledges the EU's support under H2020-MSCA-IF-2014 grant agreement 660339 (eADAM).

REFERENCES

[1] L. Jarup, Hazards of heavy metal contamination, Br. Med. Bull. 68 (2003) 167–182. doi:10.1093/bmb/ldg032.

[2] W.H. Organization, Guidelines for drinking-water quality, Fourth Ed., Geneva, 2011.

[3] C. Fernández-Bobes, M.T. Fernández-Abedul, A. Costa-García, Anodic Stripping of Heavy Metals Using a Hanging Mercury Drop Electrode in a Flow System, Electroanalysis. 10 (1998) 701–706. doi:10.1002/(SICI)1521-4109(199808)10:10<701::AID-ELAN701>3.0.CO;2-I.

[4] D. Martín-Yerga, M.B. González-García, A. Costa-García, Use of nanohybrid materials as electrochemical transducers for mercury sensors, Sens. Actuators, B. 165 (2012) 143–150. doi:10.1016/j.snb.2012.02.031.

[5] I. Álvarez-Martos, F.J. García Alonso, A. Anillo, P. Arias-Abrodo, M.D. Gutiérrez-Álvarez, A. Costa-García, M.T. Fernández-Abedul, Ionic liquids as modifiers for glass and SU-8 electrochemical microfluidic chips, Sensors Actuators B Chem. 188 (2013) 837–846. doi:10.1016/j.snb.2013.07.068.

[6] V. Castaing, I. Álvarez-Martos, E.E. Ferapontova, Wiring of Glucose Oxidizing Flavin Adenine Dinucleotide-Dependent Enzymes by Methylene Blue-Modified Third Generation Poly(amidoamine) Dendrimers Attached to Spectroscopic Graphite Electrodes, Electrochim. Acta. 197 (2016). doi:10.1016/j.electacta.2016.01.217.

[7] I. Álvarez-Martos, E.E. Ferapontova, Electrochemical Label-Free Aptasensor for Specific Analysis of Dopamine in Serum in the Presence of Structurally Related Neurotransmitters, Anal. Chem. 88 (2016) 3608–3616. doi:10.1021/acs.analchem.5b04207.

[8] A.C. Glavan, A. Ainla, M.M. Hamedi, M.T. Fernández-Abedul, G.M. Whitesides, Electroanalytical devices with pins and thread, Lab Chip. 16 (2016) 112–119. doi:10.1039/C5LC00867K.

[9] E.C. Rama, A. Costa-García, M.T. Fernández-Abedul, Pin-based electrochemical glucose sensor with multiplexing possibilities, Biosens. Bioelectron. 88 (2017) 34–40. doi:10.1016/j.bios.2016.06.068.

[10] D.M. Cate, J.A. Adkins, J. Mettakoonpitak, C.S. Henry, Recent Developments in Paper-Based Microfluidic Devices, Anal. Chem. 87 (2015) 19–41. doi:10.1021/ac503968p.

[11] J. Adkins, K. Boehle, C. Henry, Electrochemical paper-based microfluidic devices, Electrophoresis. 36 (2015) 1811–1824. doi:10.1002/elps.201500084.

[12] J. Mettakoonpitak, K. Boehle, S. Nantaphol, P. Teengam, J.A. Adkins, M. Srisa-Art, C.S. Henry, Electrochemistry on Paper-Based Analytical Devices: A Review, Electroanalysis. (2016) 1420–1436. doi:10.1002/elan.201501143.

[13] A.W. Martinez, S.T. Phillips, G.M. Whitesides, E. Carrilho, Diagnostics for the Developing World: Microfluidic Paper-Based Analytical Devices, Anal. Chem. 82 (2010) 3–10. doi:10.1021/ac9013989.

[14] W. Dungchai, O. Chailapakul, C.S. Henry, Electrochemical Detection for Paper-Based Microfluidics, Anal. Chem. 81 (2009) 5821–5826. doi:10.1021/ac9007573.

[15] Z. Nie, C. a Nijhuis, J. Gong, X. Chen, A. Kumachev, A.W. Martinez, M. Narovlyansky, G.M. Whitesides, Electrochemical sensing in paper-based microfluidic devices, Lab Chip. 10 (2010) 477–483. doi:10.1039/B917150A.

[16] M.M. Hamedi, A. Ainla, F. Güder, D.C. Christodouleas, M.T. Fernández-Abedul, G.M. Whitesides, Integrating Electronics and Microfluidics on Paper, Adv. Mater. 28 (2016) 5054–5063. doi:10.1002/adma.201505823.

[17] O. Amor-Gutiérrez, E. Costa Rama, A. Costa-García, M.T. Fernández-Abedul, Paper-based maskless enzymatic sensor for glucose determination combining ink and wire electrodes, Biosens. Bioelectron. (2016) (in press). doi:10.1016/j.bios.2016.11.008.

[18] W.-J. Lan, X.U. Zou, M.M. Hamedi, J. Hu, C. Parolo, E.J. Maxwell, P. Bühlmann, G.M. Whitesides, Paper-Based Potentiometric Ion Sensing, Anal. Chem. 86 (2014) 9548–9553. doi:10.1021/ac5018088.

[19] A.C. Glavan, D.C. Christodouleas, B. Mosadegh, H.D. Yu, B.S. Smith, J. Lessing, M.T. Fernández-Abedul, G.M. Whitesides, Folding Analytical Devices for Electrochemical ELISA in Hydrophobic R H Paper, Anal. Chem. 86 (2014) 11999–12007. doi:10.1021/ac5020782.

[20] J.C. Cunningham, N.J. Brenes, R.M. Crooks, Paper Electrochemical Device for Detection of DNA and Thrombin by Target-Induced Conformational Switching, Anal. Chem. 86 (2014) 6166–6170. doi:10.1021/ac501438y.

[21] W.R. de Araujo, T.R.L.C. Paixão, Fabrication of disposable electrochemical devices using silver ink and office paper, Analyst. 139 (2014) 2742–2747. doi:10.1039/c4an00097h.

[22] D. Tobjörk, R. Österbacka, Paper Electronics, Adv. Mater. 23 (2011) 1935–1961. doi:10.1002/adma.201004692.

[23] N. Ruecha, N. Rodthongkum, D.M. Cate, J. Volckens, O. Chailapakul, C.S. Henry, Sensitive electrochemical sensor using a graphene–polyaniline nanocomposite for simultaneous detection of Zn(II), Cd(II), and Pb(II), Anal. Chim. Acta. 874 (2015) 40–48. doi:10.1016/j.aca.2015.02.064.

[24] S. Armenta, S. Garrigues, M. de la Guardia, Green Analytical Chemistry, TrAC Trends Anal. Chem. 27 (2008) 497–511. doi:10.1016/j.trac.2008.05.003.

[25] J. Wang, J. Lu, S.B. Hocevar, P.A.M. Farias, B. Ogorevc, Bismuth-Coated Carbon Electrodes for Anodic Stripping Voltammetry, Anal. Chem. 72 (2000) 3218–3222. doi:10.1021/ac000108x.

[26] P. Niu, C. Fernández-Sánchez, M. Gich, C. Navarro-Hernández, P. Fanjul-Bolado, A. Roig, Screen-printed electrodes made of a bismuth nanoparticle porous carbon nanocomposite applied to the determination of heavy metal ions, Microchim. Acta. 183 (2016) 617–623. doi:10.1007/s00604-015-1684-4.

[27] R.O. Kadara, I.E. Tothill, Development of disposable bulk-modified screen-printed electrode based on bismuth oxide for stripping chronopotentiometric analysis of lead (II) and cadmium (II) in soil and water samples, Anal. Chim. Acta. 623 (2008) 76–81. doi:10.1016/j.aca.2008.06.010.

[28] C. Kokkinos, M. Prodromidis, A. Economou, P. Petrou, S. Kakabakos, Disposable integrated bismuth citrate-modified screen-printed immunosensor for ultrasensitive quantum dot-based electrochemical assay of C-reactive protein in human serum, Anal. Chim. Acta. 886 (2015) 29–36. doi:10.1016/j.aca.2015.05.035.

[29] M.Á. Granado Rico, M. Olivares-Marín, E. Pinilla Gil, Modification of carbon screen-printed electrodes by adsorption of chemically synthesized Bi nanoparticles for the voltammetric stripping detection of Zn(II), Cd(II) and Pb(II), Talanta. 80 (2009) 631–635. doi:10.1016/j.talanta.2009.07.039.

[30] V. Sosa, N. Serrano, C. Ariño, J.M. Díaz-Cruz, M. Esteban, Sputtered bismuth screen-printed electrode: A promising alternative to other bismuth modifications in the voltammetric determination of Cd(II) and Pb(II) ions in groundwater, Talanta. 119 (2014) 348–352. doi:10.1016/j.talanta.2013.11.032.

[31] V. Sosa, N. Serrano, C. Ariño, J.M. Díaz-Cruz, M. Esteban, Voltammetric determination of Pb(II) and Cd(II) ions in well water using a sputtered bismuth screen-printed electrode, Electroanalysis. 26 (2014) 2168–2172. doi:10.1002/elan.201400319.

[32] N. Serrano, J.M. Díaz-Cruz, C. Ariño, M. Esteban, Ex situ deposited bismuth film on screen-printed carbon electrode: A disposable device for stripping voltammetry of heavy metal ions, Electroanalysis. 22 (2010) 1460–1467. doi:10.1002/elan.200900183.

[33] N. Serrano, A. Alberich, J.M. Díaz-Cruz, C. Ariño, M. Esteban, Coating methods, modifiers and applications of bismuth screen-printed electrodes, TrAC Trends Anal. Chem. 46 (2013) 15–29. doi:10.1016/j.trac.2013.01.012.

[34] K.E. Berg, J.A. Adkins, S.E. Boyle, C.S. Henry, Manganese Detection Using Stencil-printed Carbon Ink Electrodes on Transparency Film, Electroanalysis. 28 (2016) 679–684. doi:10.1002/elan.201500474.

[35] I. Álvarez-Martos, A. Kartashov, E.E. Ferapontova, Electron Transfer in Methylene-Blue-Labeled G3 Dendrimers Tethered to Gold, ChemElectroChem. 3 (2016) 2270–2280. doi:10.1002/celc.201600417.

[36] A.J. Bard, L.R. Faulkner, Electrochemical Methods - Fundamentals and Applications, 2nd Editio, John Wiley & Sons, 2001.

[37] D. Martín-Yerga, E. Costa Rama, A. Costa García, Electrochemical Study and Determination of Electroactive Species with Screen-Printed Electrodes, J. Chem. Educ. 93 (2016) 1270–1276. doi:10.1021/acs.jchemed.5b00755.

[38] J.R. Pladziewicz, T.J. Meyer, J.A. Broomhead, H. Taube, Reduction of Oxygen by Hexaammineruthenium(II) and by Tris(ethylenediamine)ruthenium(II), Inorg. Chem. 12 (1973) 639–643. doi:10.1021/ic50121a031.

[39] P.M. Hallam, C.E. Banks, A facile approach for quantifying the density of defects (edge plane sites) of carbon nanomaterials and related structures., Phys. Chem. Chem. Phys. 13 (2011) 1210–1213. doi:10.1039/c0cp01562h.

[40] J. Wang, J. Lu, Ü.A. Kirgöz, S.B. Hocevar, B. Ogorevc, Insights into the anodic stripping voltammetric behavior of bismuth film electrodes, Anal. Chim. Acta. 434 (2001) 29–34. doi:10.1016/S0003-

2670(01)00818-2.

[41] R.T. Kachoosangi, C.E. Banks, X. JI, R.G. Compton, Electroanalytical Determination of Cadmium(II) and Lead(II) Using an in-situ Bismuth Film Modified Edge Plane Pyrolytic Graphite Electrode, Anal. Sci. 23 (2007) 283–289. doi:10.2116/analsci.23.283.

[42] V. Mirceski, S.B. Hocevar, B. Ogorevc, R. Gulaboski, I. Drangov, Diagnostics of Anodic Stripping Mechanisms under Square-Wave Voltammetry Conditions Using Bismuth Film Substrates, Anal. Chem. 84 (2012) 4429–4436. doi:10.1021/ac300135x.

[43] J. Wang, B. Tian, V.B. Nascimento, L. Angnes, Performance of screen-printed carbon electrodes fabricated from different carbon inks, Electrochim. Acta. 43 (1998) 3459–3465. doi:10.1016/S0013-4686(98)00092-9.

[44] P. Rattanarat, W. Dungchai, D. Cate, J. Volckens, O. Chailapakul, C.S. Henry, Multilayer Paper-Based Device for Colorimetric and Electrochemical Quantification of Metals, Anal. Chem. 86 (2014) 3555–3562. doi:10.1021/ac5000224.

[45] R.O. Kadara, I.E. Tothill, Resolving the copper interference effect on the stripping chronopotentiometric response of lead(II) obtained at bismuth film screen-printed electrode, Talanta. 66 (2005) 1089–1093. doi:10.1016/j.talanta.2005.01.020.

[46] D. Yang, L. Wang, Z. Chen, M. Megharaj, R. Naidu, Investigation of Copper(II) Interference on the Anodic Stripping Voltammetry of Lead(II) and Cadmium(II) at Bismuth Film Electrode, Electroanalysis. 25 (2013) 2637–2644. doi:10.1002/elan.201300375.

[47] A. Lopes Brandes Marques, G.O. Chierice, Elimination of the copper-zinc interference in anodic stripping voltammetry by addition of a complexing agent, Talanta. 38 (1991) 735–739. doi:10.1016/0039-9140(91)80193-4.

[48] R. María-Hormigos, M.J. Gismera, J.R. Procopio, M.T. Sevilla, Disposable screen-printed electrode modified with bismuth-PSS composites as high sensitive sensor for cadmium and lead determination, J. Electroanal. Chem. 767 (2016) 114–122. doi:10.1016/j.jelechem.2016.02.025.

[49] J. Shi, F. Tang, H. Xing, H. Zheng, L. Bi, W. Wang, Electrochemical detection of Pb and Cd in paper-based microfluidic devices, J. Braz. Chem. Soc. 23 (2012) 1124–1130. doi:10.1590/S0103-50532012000600018.

[50] A.A. Saeed, B. Singh, M. Nooredeen Abbas, E. Dempsey, Evaluation of Bismuth Modified Carbon Thread Electrode for Simultaneous and Highly Sensitive Cd (II) and Pb (II) Determination, Electroanalysis. 28 (2016) 2205–2213. doi:10.1002/elan.201600006.

[51] N. Lezi, A. Economou, P. a. Dimovasilis, P.N. Trikalitis, M.I. Prodromidis, Disposable screen-printed sensors modified with bismuth precursor compounds for the rapid voltammetric screening of trace Pb(II) and Cd(II), Anal. Chim. Acta. 728 (2012) 1–8. doi:10.1016/j.aca.2012.03.036.

ACCEPTED MANUSCRIPT

TABLES AND FIGURES

Table 1. Analytical figures of merit of low-cost bismuth-modified electrodes employed for Cd(II) and Pb(II) determination.

Electrodes*	Linear range (µg/L)		Sensitivity (µA L/µg)		LOD (µg/L)		Ref.
	Cd(II)	Pb(II)	Cd(II)	Pb(II)	Cd(II)	Pb(II)	
This work	1-200	1-200	0.22	0.087	0.2	0.3	
Graphene/PANI transparency electrodes	1-300	1-300	0.038	0.035	0.1	0.1	[23]
Bi/C composite SPE	1-50	1-50	0.024	0.025	1.5	2.3	[26]
Bi/PSS/SPCE	up to 45	up to 45	1.17	0.39	0.10	0.27	[48]
Paper/SPCE	10-100	10-100	0.011	0.009	2.3	2.0	[49]
Carbon micro-thread electrode	5-110	5-110	0.62	0.47	1.08	0.87	[50]
***Ex situ* Bi deposition/SPCE**	0.8 - 17.2	0.48-19.6	-	-	0.24	0.14	[30]
Bi_2O_3/SPCE	0.33-9	0.52-12.0	-	-	0.10	0.16	[30]
***In situ* Bi deposition/SPCE**	1.35-14.5	0.83-23.3	-	-	0.40	0.25	[30]
Sputtered Bi SPE	0.33 - 12.3	0.53 - 19.8	-	-	0.10	0.16	[30]
Bi citrate/SPCE	5-40	10-80	0.028	0.040	1.1	0.9	[51]

**Abbreviations: PANI: polyaniline, SPE: screen-printed electrode, PSS: polystyrene spheres, SPCE: screen-printed carbon electrodes.*

Table 2. Determination of Cd(II) and Pb(II) using the point-of-need detection system in natural water samples after spiking with 10 and 50 µg/L of each metal.

	Added (µg/L)	Found (µg/L)		Recovery (%)	
		Cd(II)	Pb(II)	Cd(II)	Pb(II)
River water	10	10.6±0.9	10±1	98-116	94-121
	50	53±2	47±2	101-110	89-97
Estuary water	10	10±1	10±1	90-114	88-105
	50	51±5	49±5	93-112	89-108

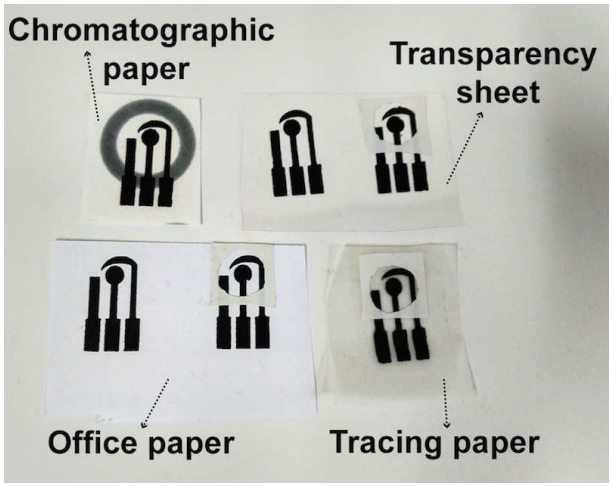

Figure 1. Picture of the different low-cost electrodes employed in this work fabricated by stencil-printing on chromatographic paper, transparency sheets, office paper and tracing paper.

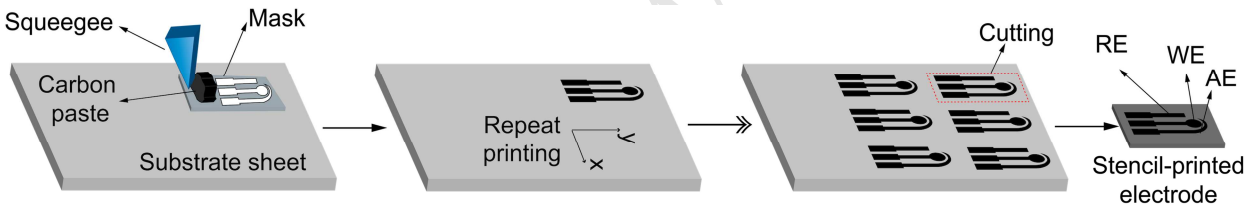

Figure 2. Schematic drawing of the stencil-printing process to fabricate several low-cost electrodes on a transparency sheet.

ACCEPTED MANUSCRIPT

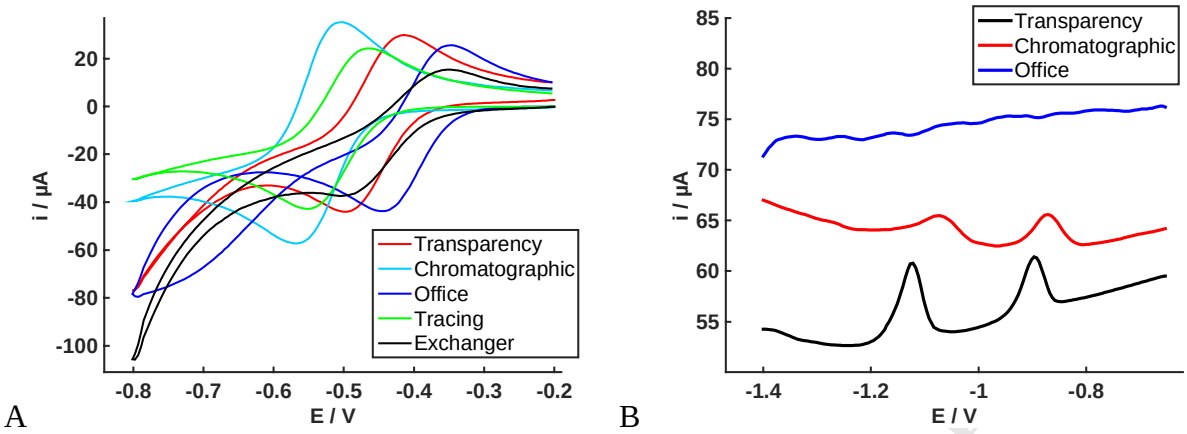

Figure 3. A) Cyclic voltammograms of 2.5 mM $[Ru(NH_3)_6]^{3+}$ in 0.1 M KCl recorded at 50 mV/s using the stencil-printed electrodes fabricated on low-cost substrates. B) Square-wave voltammograms recorded with stencil-printed electrodes for 100 µg/L of Cd(II) and Pb(II) in 0.1 M acetate buffer pH 4.5 with a preconcentration step of -1.4V, 240 s.

ACCEPTED MANUSCRIPT

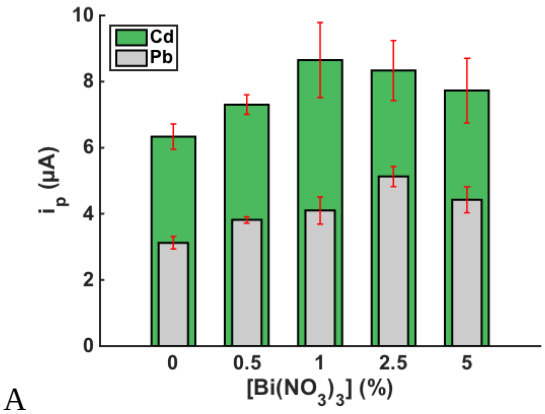

A

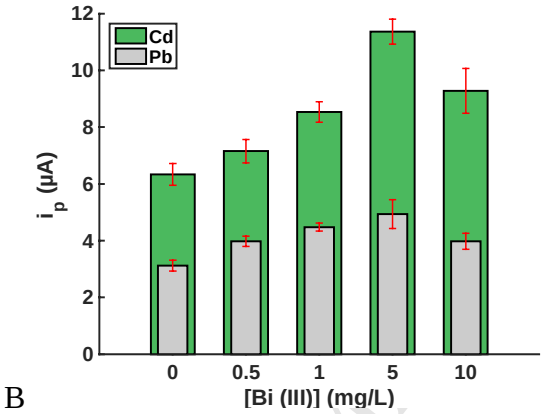

B

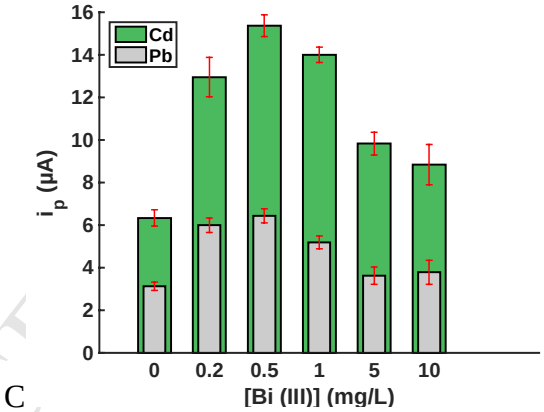

C

Figure 4. Effect of the Bi(III) concentration on the Cd(II) and Pb(II) stripping peak currents using the A) bulk, B) ex situ electrodeposition, and C) in situ electrodeposition methods to generate the bismuth film. Peak currents were obtained from the square-wave voltammograms of 100 µg/L of Cd(II) and Pb(II) in 0.1 M acetate buffer pH 4.5 with a preconcentration step of -1.4V, 240 s.

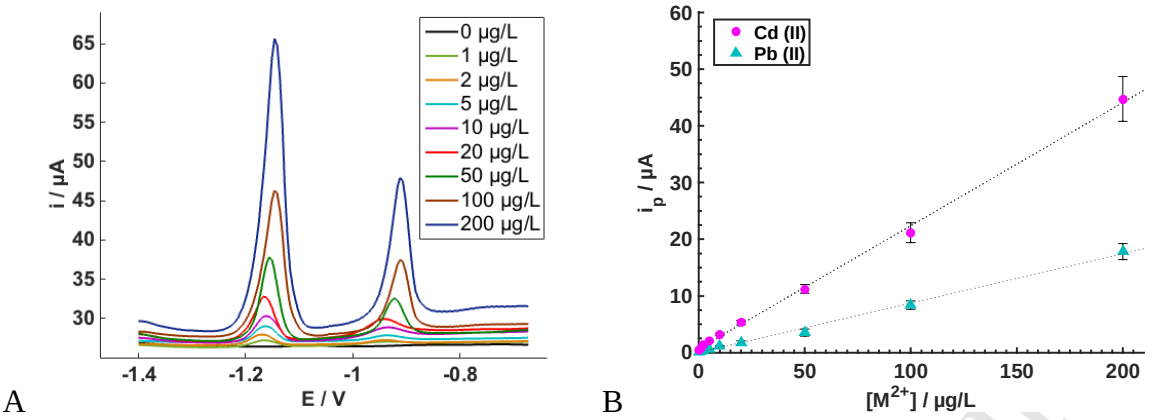

Figure 5. A) Square-wave voltammograms of Cd(II) and Pb(II) from 0-200 µg/L in 0.1 M acetate buffer pH 4.8 with *in situ* deposition of 0.5 mg/L Bi(III) using stencil-printed transparency electrodes. B) Calibration plots representing the stripping peak currents for Cd(II) and Pb(II) in relation to the metal concentration in solution.

ACCEPTED MANUSCRIPT

ACCEPTED MANUSCRIPT

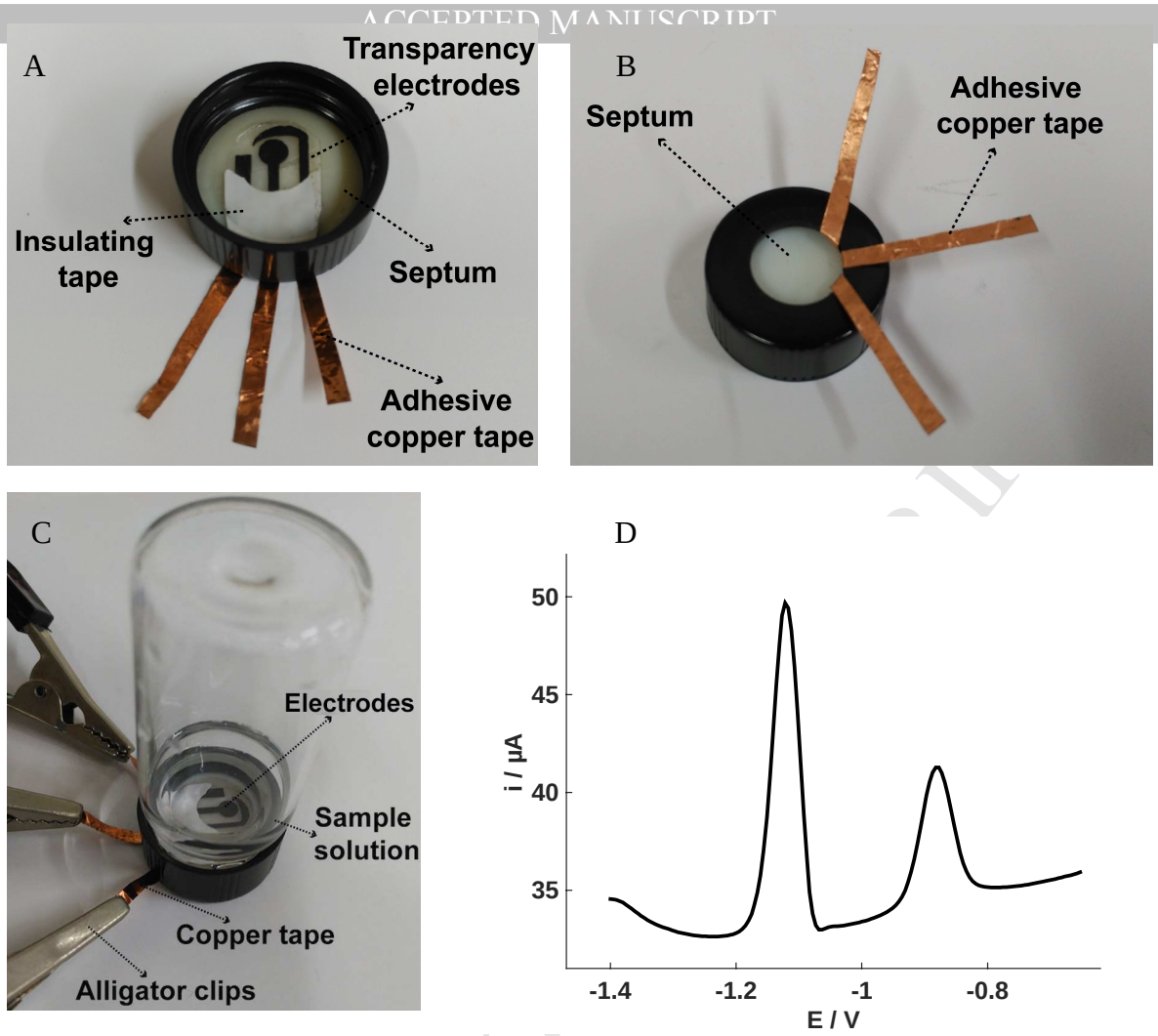

Figure 6. Picture showing the integration of the transparency electrode onto the cap of a sample vial. A) Internal side with the transparency electrodes, which is in contact with the solution and B) external side with the adhesive copper tape employed for the potentiostat connection. C) Picture of the point-of-need detection system filled with 5 mL of a sample solution and connected to the potentiostat by alligator clips. D) Square-wave voltammograms for 100 µg/L of Cd(II) and Pb(II) in 0.1 M acetate buffer pH 4.8 (10 mM citric acid) measured using the point-of-need detection system involving the integration of a transparency electrode onto the cap of a sample vial. 5 µL of 500 mg/L of a Bi(III) solution were firstly deposited (and left to evaporate) in order to obtain a solution with a 0.5 mg/L concentration of Bi(III).

ACCEPTED MANUSCRIPT

Research Highlights

- Characterized four low-cost substrates: transparency, chromatographic, tracing and office papers.
- Heavy metals showed better electrochemical performance on transparency-based electrodes.
- Capacitive current decreased notoriously when the curing time of the ink on paper was increased.
- Vial-coupled transparency electrodes allowed in field analysis of water samples.
- The limits of detection were 0.5 µg/L for Cd(II) and.4 µg/L for Pb(II).

ACCEPTED MANUSCRIPT

ACCEPTED MANUSCRIPT

SUPPORTING INFORMATION

Point-of-need simultaneous electrochemical detection of lead and cadmium using low-cost stencil-printed transparency electrodes

D. Martín-Yerga[#1], I. Álvarez-Martos[#2], M.C. Blanco-López[1], C.S. Henry[3], M.T. Fernández-Abedul*[1]*

[1] Departamento de Química Física y Analítica, Universidad de Oviedo, 33006 Oviedo, Spain

[2] Interdisciplinary Nanoscience Center (iNANO), Aarhus University, 8000 Aarhus C, Denmark

[3] Department of Chemistry, Colorado State University, Ft. Collins CO80523, USA

[#] These authors contributed equally to this work

*Corresponding authors e-mail: mtfernandeza@uniovi.es; Chuck.Henry@colostate.edu

ACCEPTED MANUSCRIPT

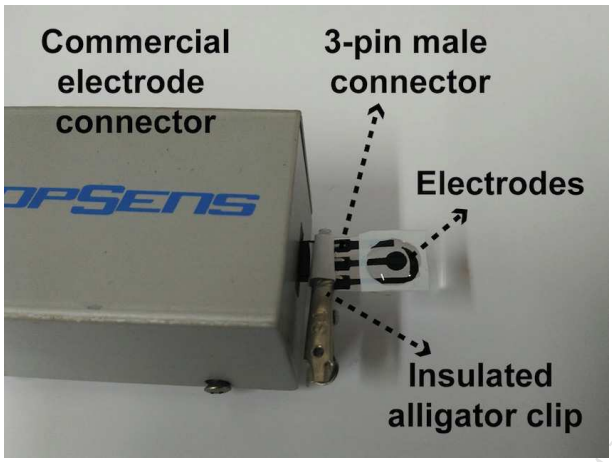

Figure S1. Picture of a transparency electrode connected to the potentiostat using a commercial connector for screen-printed electrodes and a 3-pin male connector.

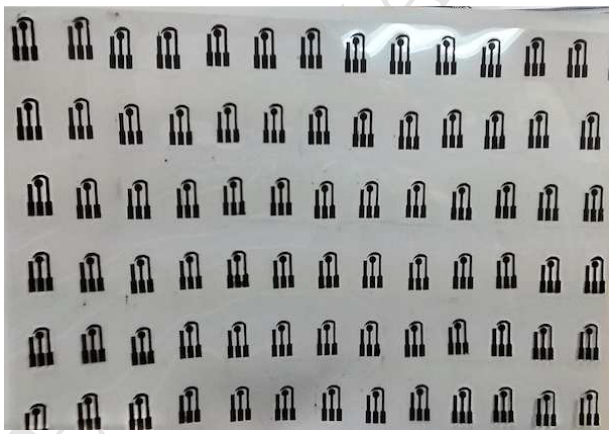

Figure S2. Picture of a transparency sheet (A4 dimensions) with tens of stencil-printed electrodes. Individual electrodes are generated by cutting the transparency sheet.

ACCEPTED MANUSCRIPT

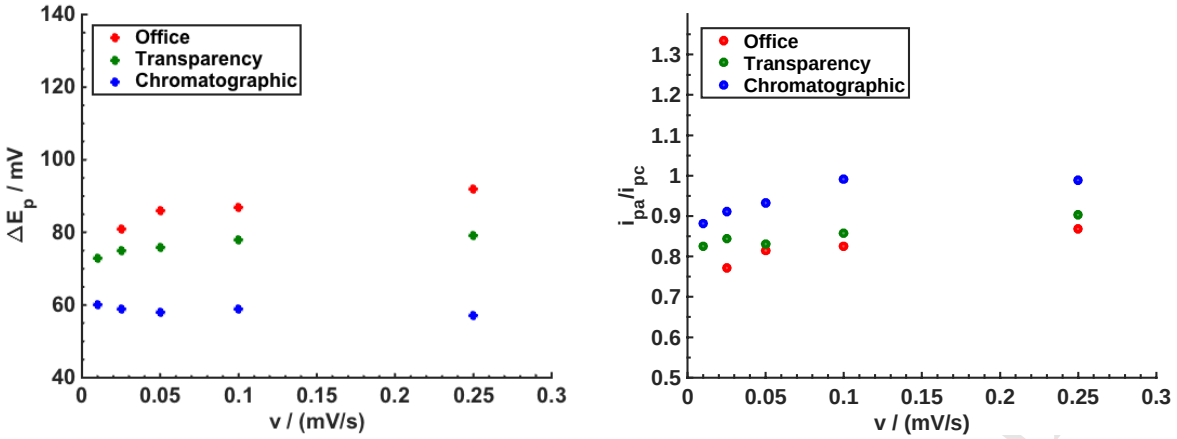

Figure S3. Variation of the peak potential difference (A) and i_{pa}/i_{pc} ratio with the scan rate of the cyclic voltammograms obtained for 2.5 mM mM $[Ru(NH_3)_6]^{3+}$ in 0.1 M KCl using electrodes fabricated on transparency sheets, chromatographic paper and office paper.

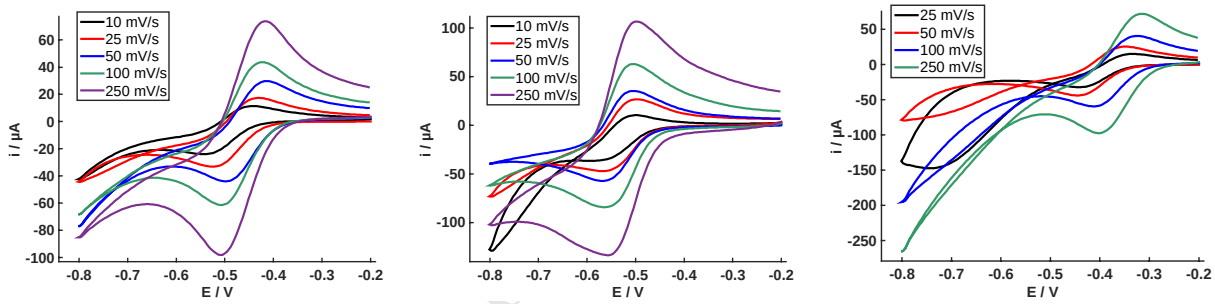

Figure S4. Cyclic voltammograms of 2.5 mM $[Ru(NH_3)_6]^{3+}$ in 0.1 M KCl at several scan rates (10, 25, 50, 100 and 250 mV/s) using the stencil-printed electrodes fabricated on transparency sheets, chromatographic paper and office paper, respectively.

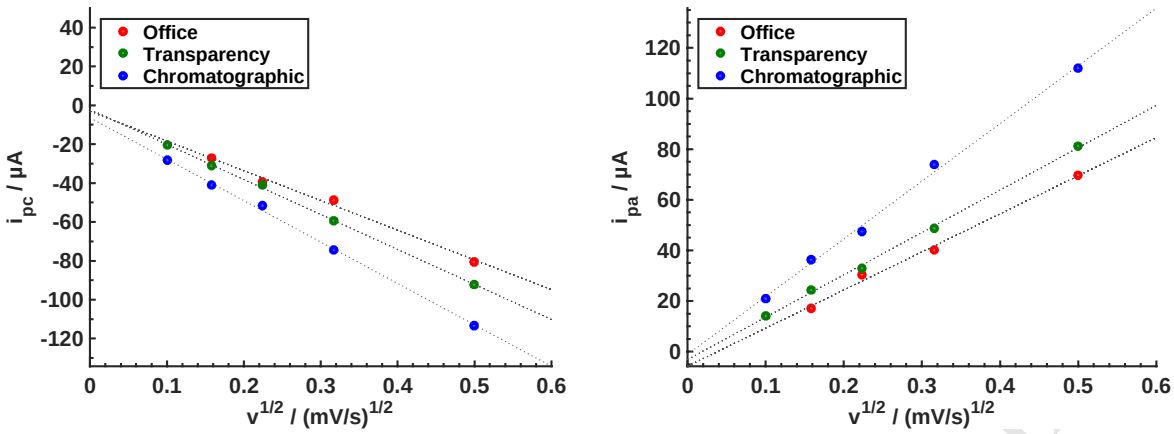

Figure S5. Anodic and cathodic peak currents variation with the square root of the scan rate of the cyclic voltammograms obtained for 2.5 mM mM $[Ru(NH_3)_6]^{3+}$ in 0.1 M KCl using electrodes fabricated on transparency sheets, chromatographic paper and office paper.

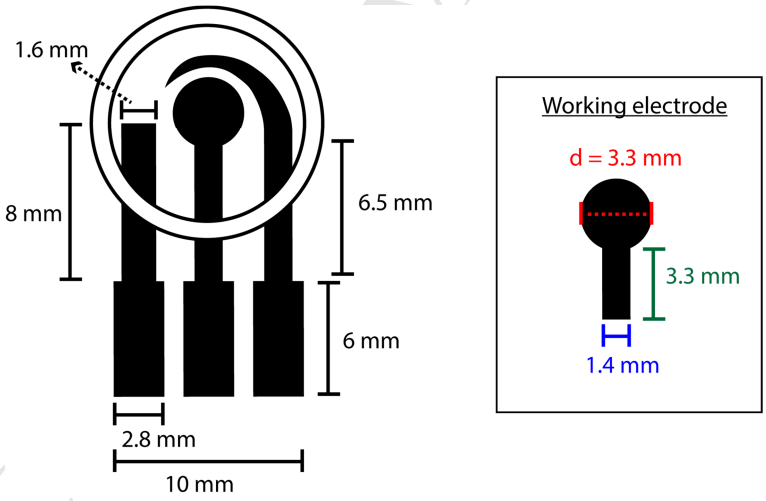

Figure S6. Schematic drawing of the dimensions of the stencil-printed electrodes. The geometric area of the working electrode was estimated using these dimensions.

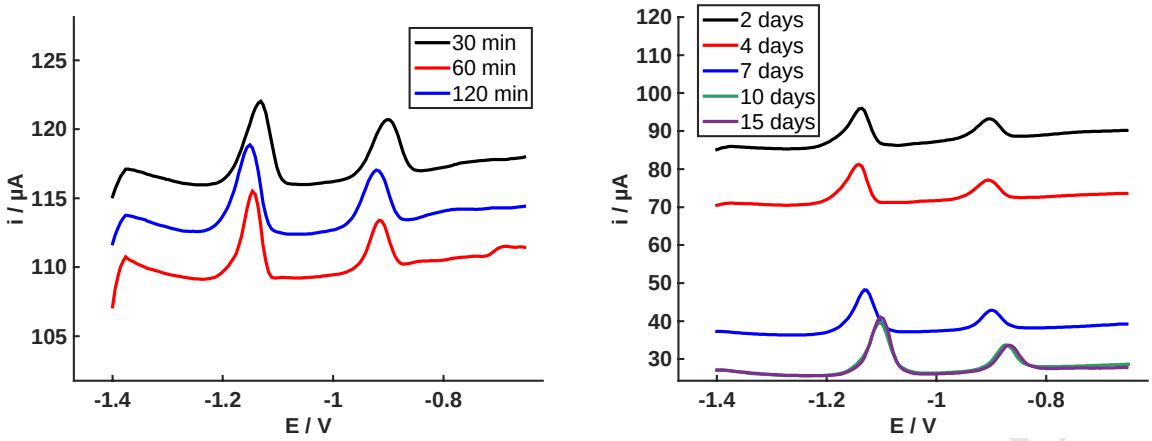

Figure S7. Effect of the curing time (at 80 ºC and 37 ºC) on the square-wave voltammograms for 100 µg/L of Cd(II) and Pb(II) in 0.1 M acetate buffer pH 4.5 measured on transparency electrodes modified with a bismuth film by the *in situ* deposition using 5 mg/L of Bi(III). Similar results were found for the curing times at 80 ºC, but significant lower capacitive currents were obtained with increasing curing times at 37 ºC.

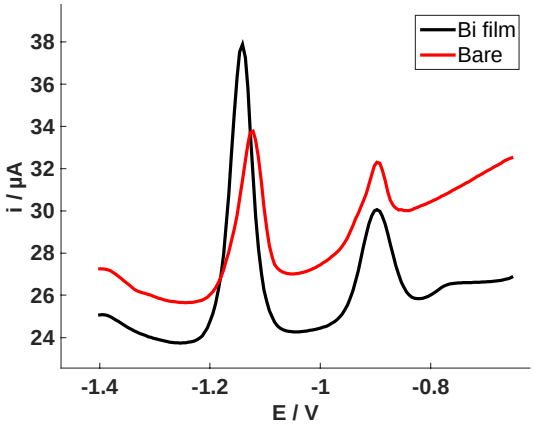

Figure S8. Square-wave voltammograms for 100 µg/L of Cd(II) and Pb(II) in 0.1 M acetate buffer pH 4.5 measured on bare transparency electrodes and modified with a bismuth film by the *in situ* deposition using 0.5 mg/L of Bi(III).

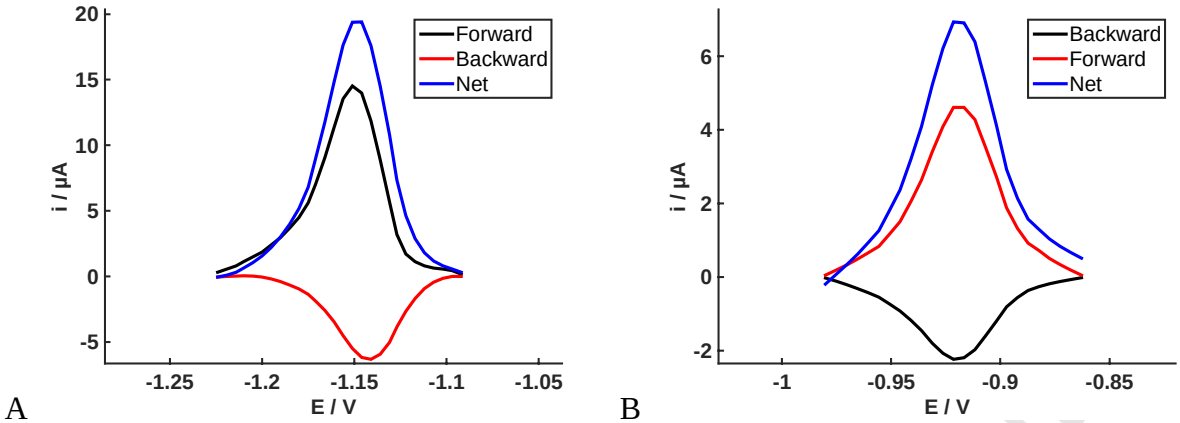

Figure S9. Net, forward and backward components of the square-wave voltammograms obtained for 100 µg/L of Cd(II) (A) and Pb(II) (B) in 0.1 M acetate buffer pH 4.8 measured on transparency electrodes modified with a bismuth film by the *in situ* deposition using a 0.5 mg/L of Bi(III). The baseline was subtracted to the responses in order to normalize the currents and be able to evaluate easily the responses obtained.

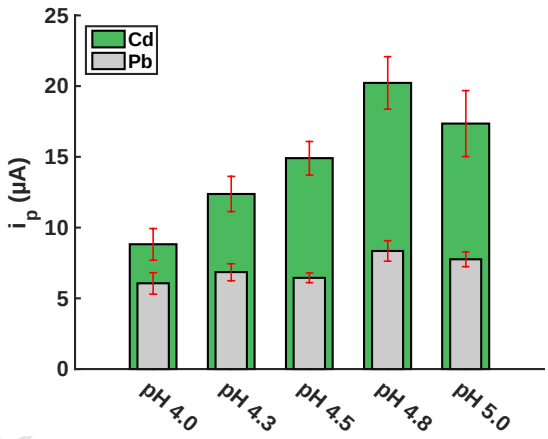

Figure S10. Effect of the acetate buffer pH on the stripping peak currents for 100 µg/L of Cd(II) and Pb(II). The stripping peak currents increased generally with increasing pH, especially for cadmium, with the optimal pH being 4.8. It seems that this pH is the most effective for the preconcentration of the metals with the Bi film, and the succeeding stripping step. Thus, pH 4.8 was chosen for the following experiments.

A B

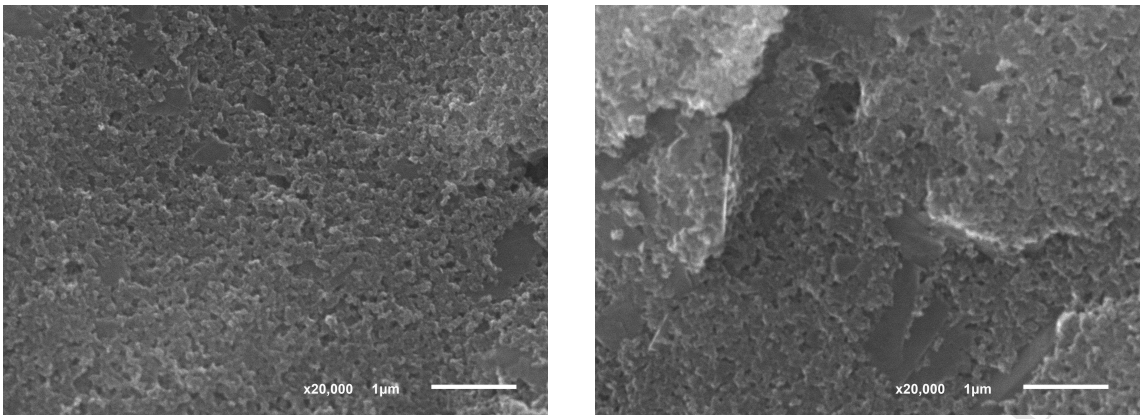

Figure S11. SEM images corresponding to transparency sheets with carbon ink cured at 37 ºC for: A)1 day and B) 15 days.

Table S1. Tolerance ratio of interfering metal ions in the electrochemical determination of 50 µg/L of Pb(II) and Cd(II) on transparency electrodes.

Interfering metal	12% Tolerance Ratio	
	Cd(II)	Pb(II)
Cu(II)	20	20
Ni(II)	100	100
Co(II)	100	50
Fe(III)	200	200
Zn(II)	200	200